Computing and Informatics, Vol. 34, 2015, 746–778

TIMED AND HYBRID PETRI NETS AT SOLVING PROBLEMS OF COMPUTATIONAL INTELLIGENCE

František Čapkovič

Institute of Informatics
Slovak Academy of Sciences
Dúbravská cesta 9
845 07 Bratislava, Slovakia
e-mail: `Frantisek.Capkovic@savba.sk`

Abstract. Timed Petri nets (TPN) and hybrid Petri nets (HPN), more precisely first-order HPN (FOHPN), are used here in order to model, analyse and control discrete-event systems (DES) and hybrid systems (HS) of different kinds consisting of cooperating subsystems (modules, agents). Foremost, principles of the particular kinds of Petri nets (PN), including the primary place/transition PN (P/T PN), are explained. Then, two methods of the supervision are introduced. Finally, the corresponding kinds of PN are applied in four case studies in order to solve the problems of modelling, analysing and control. Namely, the throughput of transport systems (rail and road), flexible manufacturing systems (FMS) and the workflow (WF) of the evacuation process from an endangered area (EA) are handled.

Keywords: Agent, computational collective intelligence, cooperation, first-order hybrid Petri nets, flexible manufacturing systems, hybrid Petri nets, place/transition Petri nets, supervision, timed Petri nets, transport systems, workflow

Mathematics Subject Classification 2010: 93-C65, 93-C30

1 INTRODUCTION AND PRELIMINARIES

Rudiments of Petri nets (PN) were built in [25]. Later, the deeper mathematical background of place/transition Petri nets (P/T PN) was elaborated, especially in [24, 28, 23, 16]. Since, P/T PN have passed through the advancement. Thus, they became the effective tool for modelling, analysing and control of discrete-event systems (DES) in general. As to their structure P/T PN are the bipartite directed graphs $\langle P, T, F, G\rangle$, where $p_i \in P$, $i = 1, \dots, n$, are the places and $t_j \in T$, $j = 1, \dots, m$, are the transitions. $F \subseteq P \times T$ is the set of the edges directed from the places to the transitions, while $G \subseteq T \times P$ is the set of the edges in the opposite direction. P/T PN have also their *dynamics* i.e. the marking evolution of their places (represented by tokens). It can be formally expressed as $\langle X, U, \delta, \mathbf{x}_0\rangle$, where X is a set of the state (marking) vectors $\mathbf{x}_k$ ($k = 0, 1, \dots$), U is a set of the state vectors $\mathbf{u}_k$ of the transitions, $\delta : X \times U \to X$ is the transition function (it indicates that discrete events change the present marking), and $\mathbf{x}_0$ is the initial state vector. δ is realized by the restricted integer linear discrete system as follows:

$$\mathbf{x}_{k+1} = \mathbf{x}_k + \mathbf{B}.\mathbf{u}_k, \quad \mathbf{B} = \mathbf{G}^T - \mathbf{F}, \quad k = 0, 1, \dots \tag{1}$$

$$\mathbf{F}.\mathbf{u}_k \leq \mathbf{x}_k. \tag{2}$$

Here, $\mathbf{x}_k = (\sigma_{p_1}, \dots, \sigma_{p_n})^T$ is the state vector, $\sigma_{p_i} \in \{0, 1, \dots\}$; $\mathbf{u}_k = (\gamma_{t_1}, \dots, \gamma_{t_m})^T$ is the vector of the states of transitions, $\gamma_{t_j} \in \{0, 1\}$, $j = 1, 2, \dots, m$, expresses whether the transition t_j is disabled (when $\gamma_{t_j} = 0$) or enabled (when $\gamma_{t_j} = 1$) i.e. allowed to be fired – namely, its firing models occurence of a discrete event; $\mathbf{B}$ expresses the P/T PN structure. Here, $\mathbf{F}$ (often **Pre**) and $\mathbf{G}^T$ (often **Post**) are the incidence matrices of the arcs corresponding, respectively, to the sets F and G. Their entries express the weights of the arcs.

P/T PN do not depend on time. Their transitions, places, arcs and tokens do not contain any time specifications. However, the extended version of P/T PN – timed Petri nets (TPN) – contain such specifications. Consequently, TPN are suitable for modelling the DES behaviour in time, especially for finding their performance evaluation and throughput. Namely, TPN directly yield the marking evolution with respect to (w.r.t.) time. In TPN certain time specifications are defined [31, 26]. Here, the time specifications are assigned exclusively to the P/T PN transitions as their duration function $D : T \to \mathbb{Q}_0^+$ ($\mathbb{Q}_0^+$ symbolizes non-negative rational numbers). Thus, P/T PN turn to TPN. There is no relation between TPN and Stochastic Petri nets here. In the deterministic case the time specifications are represented by certain time delays of the transitions, while in the non-deterministic cases they express a kind of the probability distribution of timing the transitions – exponential, discrete uniformed, Poisson's, etc.

Here, only the exponential probability distribution ${}^e f_x$ and/or the discrete uniform probability distribution ${}^u f_x$ defined as

$${}^e f_x = \begin{cases} \lambda.e^{-\lambda.x} & \text{if } x \geq 0 \\ 0 & \text{otherwise} \end{cases} \qquad {}^u f_x = \begin{cases} 1/(b-a) & \text{if } x \in (a, b) \\ 0 & \text{otherwise} \end{cases} \tag{3}$$

will be used. Namely, the simulation of the particular systems was performed in the universal simulation tool Matlab by means of the specific HYPENS toolbox developed in [29, 30], where ${}^e f_x, {}^u f_x$ are offered. The HYPENS yields the simulation results not only in mathematical form but also in the well-arranged graphical one.

Hybrid Petri nets (HPN) in general [15] are another extension of PN. HPN model the hybrid systems (HS) where discrete and continuous variables coexist. HPN have two kinds of places and two kinds of transitions – discrete and continuous. There exist four kinds of directed arcs in HPN – the arcs between:

1. discrete places and discrete transitions (expressed by $\mathbf{Pre}_{dd}$, $\mathbf{Post}_{dd}$);
2. continuous places and continuous transitions ($\mathbf{Pre}_{cc}$, $\mathbf{Post}_{cc}$);
3. discrete places and continuous transitions ($\mathbf{Pre}_{dc}$, $\mathbf{Post}_{dc}$);
4. continuous places and discrete transitions ($\mathbf{Pre}_{cd}$, $\mathbf{Post}_{cd}$).

While the HPN discrete places and transitions handle the discrete tokens, the HPN continuous places and transitions handle the continuous variables (flows). First-order HPN (FOHPN) are a simplified (but mathematically improved) kind of HPN. FOHPN are comprehensively defined in details in [3, 4, 5, 17, 29]. Here, $P = P_d \cup P_c$, where P_d is a set of the discrete places (figured by circles) and P_c is a set of the continuous places (figured by double concentric circles). $T = T_d \cup T_c$, where T_d is a set of the discrete transitions (figured by rectangles) and T_c is a set of the continuous transitions (figured by double rectangles). T_d contains a subset of the immediate (no timed) transitions and/or a subset of the timed transitions (deterministic and/or non-deterministic). There are two kinds of marking in FOHPN:

1. the discrete marking expressed by the tokens in the discrete places;
2. the continuous marking expressed by an amount of a substance (fluid) in the continuous places.

The instantaneous firing speed (IFS) $V_j^{min} \leq v_j(\tau) \leq V_j^{max}$ [3, 4, 5], determining an amount of the substance per time unit in a time instant τ, is assigned to each of the continuous transition T_j. The marking development of the continuous place $P_i \in P_c$ in time can be described by the differential equation $dM_i/d\tau = \sum_{T_j \in T_c} C(P_i, T_j).v_j(\tau)$, where $v_{j\in\langle 1,n_c\rangle}(\tau)$ are entries of the IFS vector $\mathbf{v}(\tau) = (v_1(\tau), \ldots, v_{n_c}(\tau))^T$ in the time τ and $\mathbf{C} = \mathbf{Post}_{cc} - \mathbf{Pre}_{cc}$. The continuous transition T_j is enabled in the time instant τ [3, 4, 5, 29] if and only if:

1. its input discrete places $p_k \in P_d$ have the marking $m_k(\tau)$ at least equal to the element $Pre_{dc}(p_k, T_j)$ of the incidence matrix $\mathbf{Pre}_{dc}$;
2. and all of its input continuous places $P_i \in P_c$ satisfy the condition that their markings $M_i(\tau) \geq 0$ – i.e. the places P_i are filled.

Namely, T_j cannot take more fluid from any empty input continuous place than the volume entering the place from its input transitions. This corresponds to the principle of the mass conservation. For the so called well-formed FOHPN [5] holds $\mathbf{Pre}_{dc} = \mathbf{Post}_{dc}$. More details are in [3, 4, 5].

By Workflow (WF) [1, 2] we mean a series of activities which are necessary to complete a given task. WF has the character of DES. Thus, WF is often modelled by means of P/T PN. Also some WF problems can be solved by P/T PN.

Modelling, analysing and control of MAS by means of P/T PN were pointed out e.g. in [6, 7] and applied in [8, 9, 12, 14] to the evacuation process, in [10, 13] to the road transport systems and in [11] to the logistics. The results presented there represent the starting point for the development performed in this paper, based on TPN and FOHPN. The case studies from four important areas of practice are introduced here:

1. finding the throughput of the rail tracks;
2. finding the suitable travel routes at the increased traffic density (because of the bounded traffic or congestion) in the road transport system;
3. finding the throughput of a kind of flexible manufacturing systems (FMS);
4. finding WF of the evacuation of humans from an endangered area (EA).

2 P/T PN-BASED SUPERVISION

P/T PN are the simplest but mathematically well-described kind of PN. Due to the linearity (2), there exist many methods in analytical terms for testing P/T PN properties, reachability of states, place/transition invariants, supervision, etc.

2.1 Supervision Based on P-Invariants

Due to the specific character of DES, the methods used in classical control theory cannot be applied for the synthesis of their control. To reach desired behaviour of DES, only the supervision in virtue of prescribed conditions can be used. The P-invariants of the P/T PN model play very important role at the supervisor synthesis [18, 19, 20, 7, 9]. They are defined as the vectors $\mathbf{w}$ satisfying the condition

$$\mathbf{w}^T.\mathbf{x}_k = \mathbf{w}^T.\mathbf{x}_0 \tag{4}$$

for each state vector $\mathbf{x}_k$ reachable from the initial state vector $\mathbf{x}_0$. After evolving according to (1) the following relation arises

$$\begin{aligned} \mathbf{x}_k &= \mathbf{x}_{k-1} + \mathbf{B}.\mathbf{u}_{k-1} = \mathbf{x}_{k-2} + \mathbf{B}.(\mathbf{u}_{k-1} + \mathbf{u}_{k-2}) = \dots \\ &= \mathbf{x}_0 + \mathbf{B}.(\mathbf{u}_0 + \mathbf{u}_1 + \dots + \mathbf{u}_{k-1}) = \mathbf{x}_0 + \mathbf{B}.\mathbf{v}, \end{aligned} \tag{5}$$

where $\mathbf{v}$ is named as the Parikh's vector. It yields information on how many times the particular transitions are fired during the evolution of P/T PN from the initial state $\mathbf{x}_0$ to a prescribed terminal state $\mathbf{x}_k$. Thus, the condition (4) acquires the form

$$\mathbf{w}^T.\mathbf{B}.(\mathbf{u}_0 + \mathbf{u}_1 + \dots + \mathbf{u}_{k-1}) = \mathbf{w}^T.\mathbf{B}.\mathbf{v} = \mathbf{0}. \tag{6}$$

Because in general $\mathbf{v} \neq \mathbf{0}$, the term $\mathbf{w}^T.\mathbf{B} = \mathbf{0}$. This is an alternative definition of the P-invariants. For more invariants the vector $\mathbf{w}$ acquires the form of the matrix of the invariants $\mathbf{W}$. Hence,

$$\mathbf{W}^T.\mathbf{B} = \mathbf{0}. \tag{7}$$

In order to synthesize the supervisor, let us force the suitable restrictive condition on the state vectors in the following generalized form

$$\mathbf{L}_p.\mathbf{x} \leq \mathbf{b}, \tag{8}$$

where $\mathbf{L}_p$ is an integer matrix with the dimensionality $(n_s \times n)$ and $\mathbf{b}$ is an integer vector of limitations with the dimensionality $(n_s \times 1)$. In order to eliminate the inequality in (8) insert there the $(n_s \times 1)$ vector $\mathbf{x}_s$ of *slack* variables. Thus,

$$\mathbf{L}_p.\mathbf{x} + \mathbf{x}_s = \mathbf{L}_p.\mathbf{x} + \mathbf{I}_s.\mathbf{x}_s = (\mathbf{L}_p\mathbf{I}_s).\begin{pmatrix} \mathbf{x} \\ \mathbf{x}_s \end{pmatrix} = \mathbf{b}, \tag{9}$$

where $\mathbf{I}_s$ is the $(s \times s)$ identity matrix. To synthesize the supervisor with a structure $\mathbf{B}_s$ (so far unknown), force the matrix $(\mathbf{L}_p, \mathbf{I}_s)$ into (7) instead of $\mathbf{W}^T$ and the matrix $(\mathbf{B}^T, \mathbf{B}_s^T)^T$ instead of $\mathbf{B}$. Hence, the structure of the supervisor was found as

$$(\mathbf{L}_p\mathbf{I}_s).\begin{pmatrix} \mathbf{B} \\ \mathbf{B}_s \end{pmatrix} = \mathbf{0}; \quad \mathbf{B}_s = -\mathbf{L}_p.\mathbf{B}; \quad \mathbf{B}_s = \mathbf{G}_s^T - \mathbf{F}_s, \tag{10}$$

where $\mathbf{B}_s$ represents the interconnections of n_s additional places (called *monitors*) with the original PN. $\mathbf{F}_s, \mathbf{G}_s$ obtained by the decomposition of $\mathbf{B}_s$ are the incidence matrices of the directed arcs. The monitors together with the arcs create the supervisor. The initial state of the supervisor follows from (9) in the form $\mathbf{x}_s^0 = \mathbf{b} - \mathbf{L}_p.\mathbf{x}_0$.

To illustrate the previous procedure, consider two modules given in Figure 1 (left). When e.g. p_2, p_4 model two devices which share one *source* (e.g. a working space, a power source, a track, etc.), their activities are limited by the condition $\sigma_{p_2} + \sigma_{p_4} \leq 1$. It means that p_2, p_4 cannot possess the token simultaneously, but only alternately. It is the mutual exclusion. Satisfying this condition the supervisor S given in Figure 1 (right) can be synthesized. Namely, $\mathbf{L}_p = (0, 1, 0, 1)$, $\mathbf{b} = 1$, $n_s = 1$, $n = 4$, $m = 4$. $\mathbf{B}$ and $\mathbf{x}_0$ are displayed in Figure 1 as well as $\mathbf{B}_s$, $\mathbf{F}_s$, $\mathbf{G}_s^T$ and $\mathbf{x}_s^0$.

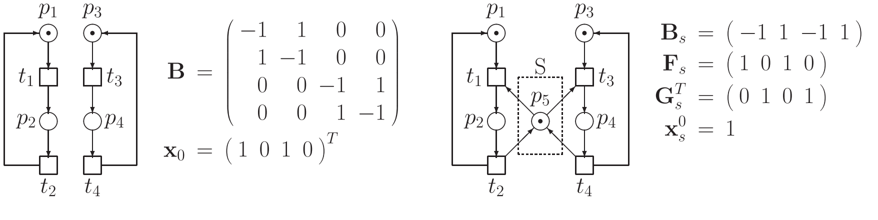

Figure 1. The supervision of two modules sharing one source

2.2 The Generalized Supervision

While in the previous supervision method the constraints were imposed only on the state vector $\mathbf{x}$, here they are imposed also on the control vector $\mathbf{u}$ and the Parikh's vector $\mathbf{v}$. Namely,

$$\mathbf{L}_p.\mathbf{x} + \mathbf{L}_t.\mathbf{u} + \mathbf{L}_v.\mathbf{v} \leq \mathbf{b}, \tag{11}$$

where $\mathbf{L}_t, \mathbf{L}_v$ are $(n_s \times m)$ matrices of integers. It was proved in [20] that when $\mathbf{b} - \mathbf{L}_p.\mathbf{x}_0 \geq \mathbf{0}$ the supervisor with the following parameters

$$\begin{aligned} \mathbf{F}_s &= \max(\mathbf{0}, \mathbf{L}_p.\mathbf{B} + \mathbf{L}_v, \mathbf{L}_t), & (12)\\ \mathbf{G}_s^T &= \max(\mathbf{0}, \mathbf{L}_t - \max(\mathbf{0}, \mathbf{L}_p.\mathbf{B} + \mathbf{L}_v)) - \min(\mathbf{0}, \mathbf{L}_p.\mathbf{B} + \mathbf{L}_v), & (13)\\ {}^s\mathbf{x}_0 &= \mathbf{b} - \mathbf{L}_p.\mathbf{x}_0 - \mathbf{L}_v.\mathbf{v}_0 & (14) \end{aligned}$$

guarantees that the constraints are verified for the states resulting from the initial state $\mathbf{x}_0$. Here, $\mathbf{0}$ is the zero matrix, $\mathbf{v}_0$ is the initial Parikh's vector and the max(.)/min(.) is the maximum/minimum operator for matrices. It is applied on matrices element-by-element.

The Parikh's vector is crucial especially at the determination of priorities among firing the P/T PN transitions. Then, the simplified condition (11) in the form

$$\mathbf{L}_v.\mathbf{v} \leq \mathbf{b} \tag{15}$$

has to be imposed. Thus, the incidence matrices of the supervisor and its initial state are the following

$$\begin{aligned} \mathbf{F}_s &= \max(\mathbf{0}, \mathbf{L}_v), & (16)\\ \mathbf{G}_s^T &= \max(\mathbf{0}, -\max(\mathbf{0}, \mathbf{L}_v)) - \min(\mathbf{0}, \mathbf{L}_v), & (17)\\ \mathbf{x}_s^0 &= \mathbf{b} - \mathbf{L}_v.\mathbf{v}_0. & (18) \end{aligned}$$

Although on the one hand P/T PN possess the sophisticated mathematical background, on the other hand, they are not able to express the time relations. In spite of this disadvantage, P/T PN are very useful for preparing the final TPN models as well as the discrete parts of the FOHPN models. In our case it is sufficient to assign the time specifications to the P/T PN transitions and the TPN model arises. The same is valid for the discrete part of the FOHPN model.

3 CASE STUDY ON RAIL TRANSPORT

The railway transport has the character of DES. Let us introduce the simple example of a circular rail network consisting of 5 mutually interconnecting tracks as in Figure 2. Tr_i, $i = 1, \ldots, 5$, mean the particular tracks while St_i, $i = 1, \ldots, 5$, mean the particular switches or stations. Of course, the number of tracks can be larger or smaller than 5. The individual tracks can be understood to be the passive agents – the agents without own goals [21]. Each agent has three states: p_1 – free; p_2 – a train claims for the access to it; p_3 – busy. The train can move to another track only if it has successfully claimed for it [2]. The P/T PN model of the circular network with five tracks is given in Figure 4.

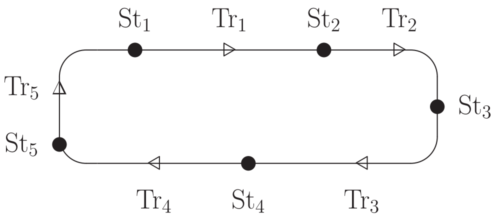

Figure 2. The circle railway with five tracks

To answer the natural question how such a model was built, let us start with the interconnection and/or cooperation of two tracks.

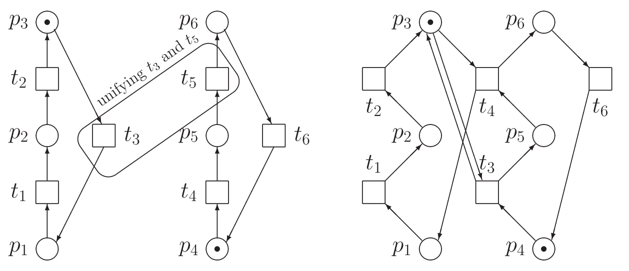

Figure 3. The P/T PN model of two individual tracks and their connection

The P/T PN model of two adjacent agents is in Figure 3 (left). The first step to the agent cooperation is unifying the transitions t_3 and t_5. Thus, the new transition t_4 arises. Other transitions of the second agent have also to be renamed. Then, from the right part of Figure 3 it is clear that:

1. t_3 is enabled because p_3 (representing the busy track Tr$_1$) and p_4 (representing the free track Tr$_2$) are active such that the transition t_3 can be fired and consequently p_5 turns to active;
2. simultaneously, the loop $p_3 \leftrightarrow t_3$ ensures the continuation of the activity of p_3;
3. thus, t_4 is enabled because the places p_3 and p_5 (representing the demand to get into the track Tr$_2$) are active;
4. consequently, after firing t_4 the place p_6 (representing the busy track Tr$_2$) becomes active while p_3 gets passive.

After extending the number of tracks to five we have the P/T PN model given in Figure 4. Here, three trains are considered to be in the network simultaneously.

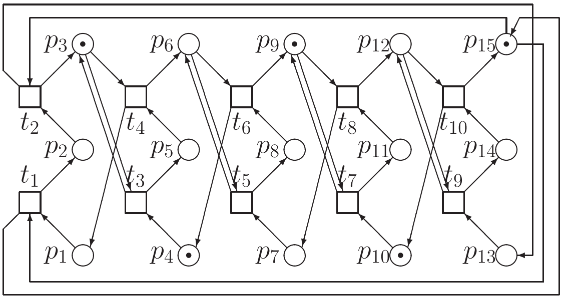

Figure 4. The P/T PN-based model of the circular rail network with five tracks where three tracks are busy (occupied by trains)

To ensure the circularity of the railway, the 5$^{\text{th}}$ track is interconnected with the 1$^{\text{st}}$ one. The reachability tree (RT) of the model for the initial state $\mathbf{x}_0 = (0,0,1,1,0,0,0,0,1,1,0,0,0,0,1)^T$ is given in Figure 5 (left) while the corresponding reachability graph (RG) is in Figure 5 (right).

RT represents the space of the feasible states – i.e. the states reachable from the initial state $\mathbf{x}_0$. Its form and size depend on the number n_t of the tracks in the circle. For the circle railway with $n_t = 2$, the number of the RT nodes is $n_{RTnodes} = 4$. The RT has the form $\mathbf{x}_0 \xrightarrow{t_3} \mathbf{x}_1 \xrightarrow{t_4} \mathbf{x}_2 \xrightarrow{t_1} \mathbf{x}_3 \xrightarrow{t_2} \mathbf{x}_0$. For $n_t = 3$, $n_{RTnodes} = 6$ and RT is: $\mathbf{x}_0 \xrightarrow{t_3} \mathbf{x}_1 \xrightarrow{t_4} \mathbf{x}_2 \xrightarrow{t_1} \mathbf{x}_3 \xrightarrow{t_2} \mathbf{x}_4 \xrightarrow{t_5} \mathbf{x}_5 \xrightarrow{t_6} \mathbf{x}_0$. However, for $n_t = 4$, $n_{RTnodes} = 16$, for $n_t = 5$, $n_{RTnodes} = 30$, for $n_t = 6$, $n_{RTnodes} = 76$, etc. Moreover, branching occurs in such RTs. The RT edges denoted by the PN transitions show how the states of the P/T PN can evolve. Connecting the repeated RT nodes (i.e. the nodes with the same name) into one node we obtain the RG. The feasible trajectories starting from the given initial state to a prescribed terminal one can be extracted from RG [7]. Each trajectory successively passes from the existing state of P/T PN to the next state. For the RT in Figure 5 (left) the cyclic trajectories (starting and ending in $\mathbf{x}_0$) lie in Figure 5 (right) inside of the dashed area. In general, in such a case we are speaking about the *working cycle*. There are 160 possible trajectories of the length 10 steps given in Figure 5 (right). However, not all of the states occurring in RT and/or RG have to appear in the trajectories. As it can be seen in Figure 5 (right), the states $\mathbf{x}_{24}$, $\mathbf{x}_{27} - \mathbf{x}_{29}$ of the RT are not involved in the *working cycles*.

Let us utilize the TPN model in order to find the performance evaluation and throughput of the tracks. Consider five tracks and three trains. Let the initial state be the same as that introduced in Figure 4. Assign the following deterministic time delays (in time unit) to the particular transitions: $\tau_{t_1} = 1.5$, $\tau_{t_2} = 12$, $\tau_{t_3} = 2.5$, $\tau_{t_4} = 15$, $\tau_{t_5} = 2$, $\tau_{t_6} = 13$, $\tau_{t_7} = 1.8$, $\tau_{t_8} = 14$, $\tau_{t_9} = 2.5$, $\tau_{t_{10}} = 15$. The corresponding marking evolution of the particular TPN places in time (obtained by HYPENS [29, 30]) is displayed in Figure 6.

The graphical outputs of the simulation experiments with TPN model make possible to find the throughput of the railway network almost exactly. Even, the model

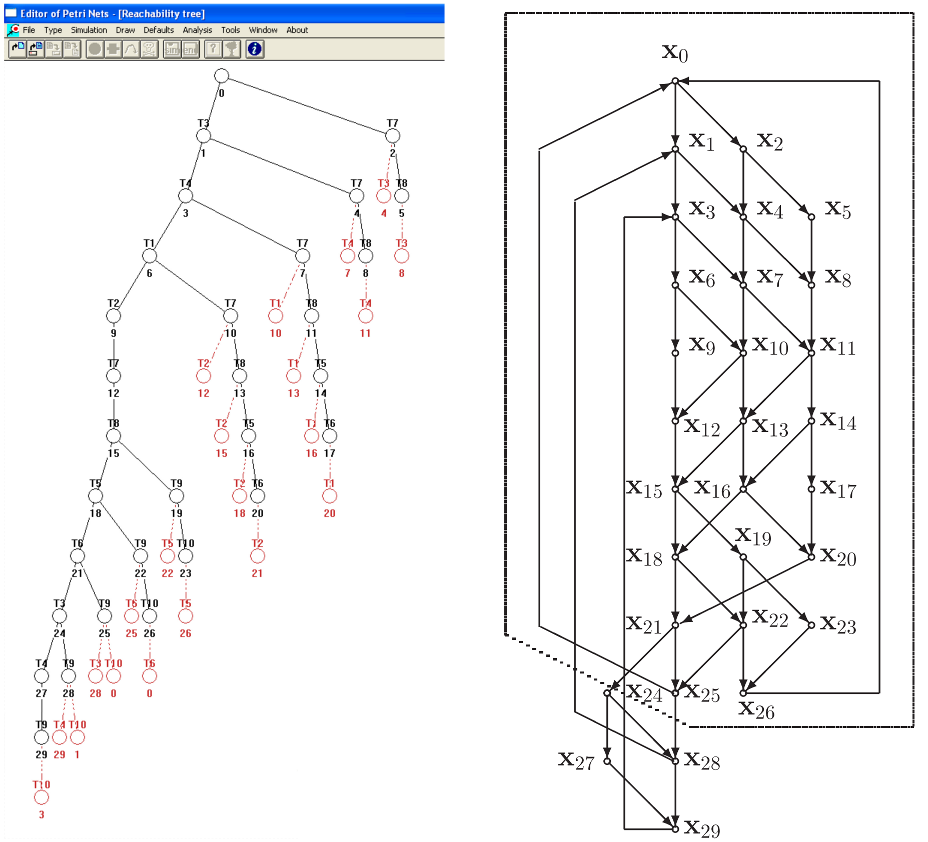

Figure 5. The RT of the five tracks P/T PN model corresponding to the initial state $\mathbf{x}_0 = (0, 0, 1, 1, 0, 0, 0, 0, 1, 1, 0, 0, 0, 0, 1)^T$ (left) and RG accordant with RT (right)

can be arbitrarily supervised. This makes possible to study different structures of the model by means of simulation.

As it follows from Figure 4, there are two possibilities how to start the process of sharing the tracks. Namely, the transitions t_3 and t_7 are enabled. When t_3 is fired, the track Tr_2 is activated (a train can enter this track). However, when t_7 is fired, the track Tr_4 is activated. The supervisor (16)–(18) based on the Parikh's vector $\mathbf{v}$ decides on the priority by virtue of (15). When it is useful e.g. to start t_7 before t_3 (i.e. $v_7 > v_3$, hence $v_3 - v_7 < 0$), the matrix $\mathbf{L}_v$ acquires the form $\mathbf{L}_v = (0, 0, 1, 0, 0, 0, -1, 0, 0, 0)$. When $\mathbf{v}_0 = \mathbf{0}$ and $\mathbf{b} = 0$, the supervisor structure and initial state have the form $\mathbf{F}_s = (0, 0, 0, 0, 0, 0, 1, 0, 0, 0)$, $\mathbf{G}_s^T = (0, 0, 1, 0, 0, 0, 0, 0, 0, 0)$, $\mathbf{x}_s^0 = 0$. It means that the supervisor consists of the additional place p_{16} (it has to be added to the Figure 4) which is initially passive (without tokens). Its output arc leads to t_3 and its input arc starts from t_7. In the

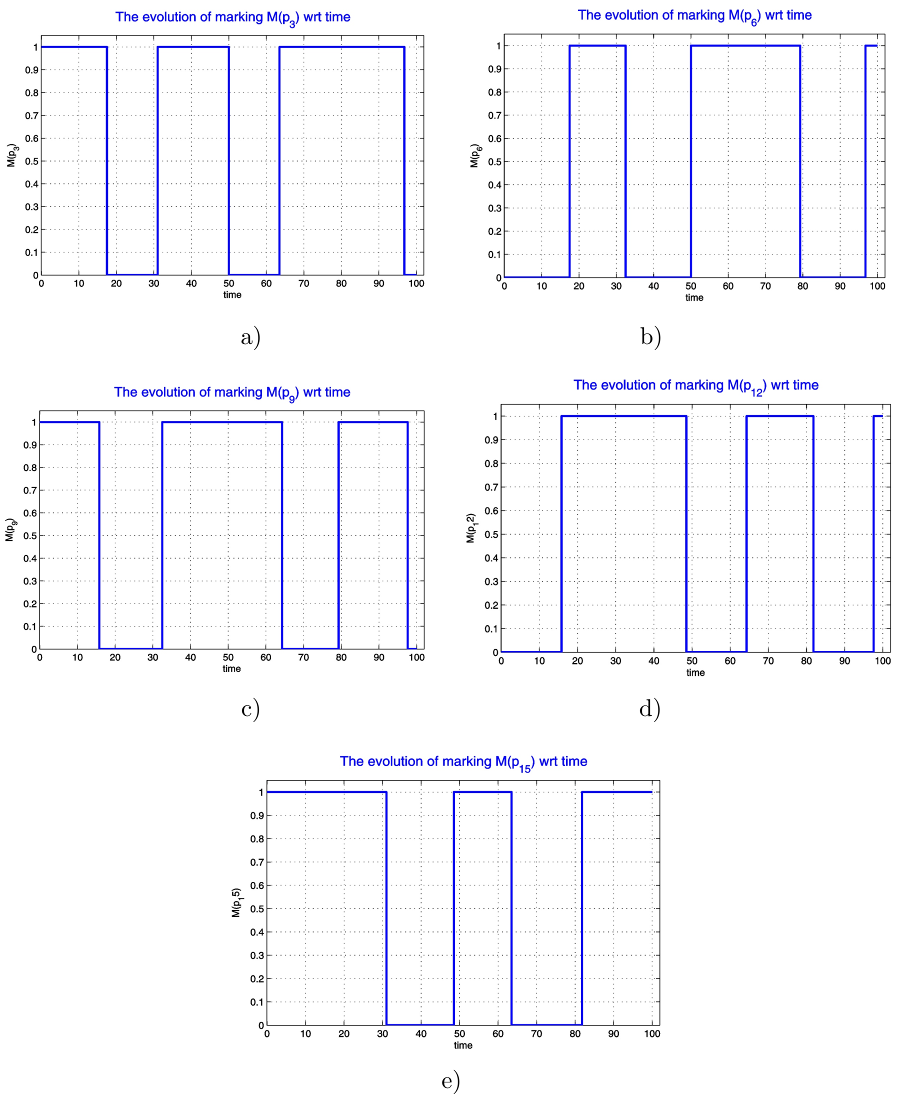

Figure 6. The performance evaluation and the throughput of the circular railway network with 5 tracks and 3 trains by means of the TPN model. The marking evolution of the corresponding TPN places w.r.t. time: p_3 in picture a) represents the throughput of the first track, while p_6 in b), p_9 in c), p_{12} in d) and p_{15} in e) represent, respectively, the throughput of the second, third, fourth and fifth tracks.

case, when the original model is supervised by the supervisor, the priority between the transitions is guaranteed. Moreover, the number of the feasible states is reduced to 22 and all of 61 trajectories of the supervised system are the *working cycles*.

4 CASE STUDY ON ROAD TRANSPORT

Pay now the attention to the road transport. In this kind of the transport systems the traffic congestion causes many specific problems. Let us build the FOHPN model of a real situation [27] displayed in Figure 7. The numbers in the circles express the locations in a street network in a city or in a road network in the countryside. The FOHPN model is in Figure 8, where the places P_i, $i = 1, \ldots, 8$, represent the locations while the transitions T_j, $j = 1, \ldots, 11$, represent the roads among the locations.

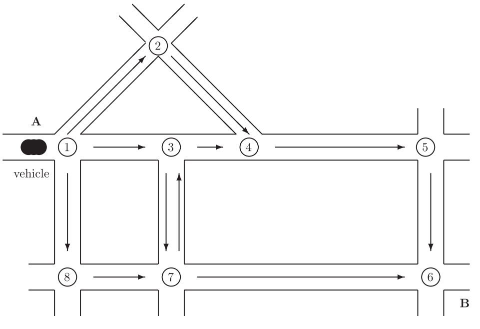

Figure 7. The scenario of the road traffic system

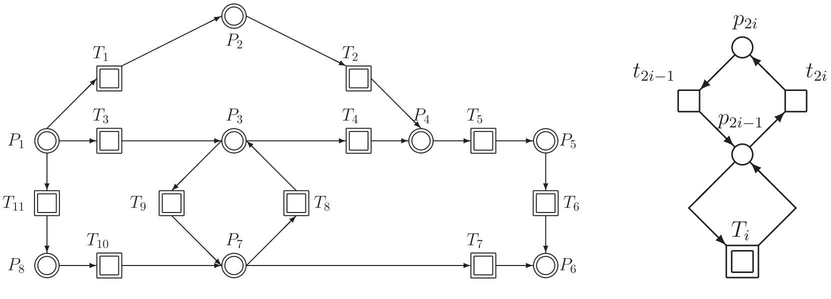

Figure 8. The FOHPN model of the scenario (left) and the TPN sub-net for controlling the continuous transitions T_i, $i = 1, \ldots, 11$, of the FOHPN model (right)

Let us observe the movement of the vehicles from the location A (P_1) to B (P_6). Denote the distances between the corresponding locations as d_{ik}, $i, k = 1, \ldots, 8$, in a length unit. Assume that $d_{12} = 40$, $d_{24} = 30$, $d_{13} = 30$, $d_{34} = 20$, $d_{45} = 50$, $d_{56} = 30$, $d_{76} = 30$, $d_{73} = 40$, $d_{37} = 40$, $d_{87} = 40$, $d_{18} = 30$. The traffic flows on the roads usually vary as well as time needed for passing the routes. In [22] the approach called as the Adaptive Gray Threshold Traffic Parameters Measurement (AGTTPM) for extracting the traffic parameters (such as traffic flow and average vehicle speed) from real traffic data was proposed. Consider that data about the average vehicle speed of each road section (because of a kind of congestion) are at disposal from the AGTTPM system. Then, such information can be used in order to compute average travel time for each road section. Assume that $v_{12} = 10$, $v_{24} = 5$, $v_{13} = 5$, $v_{34} = 5$, $v_{45} = 10$, $v_{56} = 10$, $v_{76} = 3.33$, $v_{73} = 10$, $v_{37} = 5$, $v_{87} = 10$, $v_{18} = 10$. These speeds can be utilized at defining the limits of the FOHPN speeds (IFS). However, estimated travel time τ_{ij} can be computed as the ratio of the distance d_{ij} to the average vehicle speed v_{ij}. Hence, $(\tau_{12} = 4) \to t_1$, $(\tau_{24} = 6) \to t_2$, $(\tau_{13} = 6) \to t_3$, $(\tau_{34} = 4) \to t_4$, $(\tau_{45} = 5) \to t_5$, $(\tau_{56} = 3) \to t_6$, $(\tau_{76} = 9) \to t_7$, $(\tau_{73} = 4) \to t_8$, $(\tau_{37} = 8) \to t_9$, $(\tau_{87} = 4) \to t_{10}$, $(\tau_{18} = 3) \to t_{11}$. Such a TPN-based approach was used in [10] so that the most suitable routes during the traffic congestion were flexibly found. Here, the FOHPN model is used in order to observe the flows of vehicles from the selected initial location towards the desired terminal one. Each continuous transition T_i, $i = 1, \dots, 11$, of the FOHPN model is controlled by the discrete TPN sub-net given in Figure 8 (right). Meaning of the discrete places and transitions is the following:

1. if the discrete place p_{2i-1} is active then T_i is open;
2. if the discrete place p_{2i-1} is passive then T_i is closed.

The discrete transitions t_{2i-1}, t_{2i} may be either deterministic (with the time delays) or non-deterministic (with a probability distribution of timing). The structural parameters of the FOHPN continuous part are as follows:

$$\mathbf{Pre}_{cc} = \begin{pmatrix} 1 & 0 & 1 & 0 & 0 & 0 & 0 & 0 & 0 & 0 & 1 \\ 0 & 1 & 0 & 0 & 0 & 0 & 0 & 0 & 0 & 0 & 0 \\ 0 & 0 & 0 & 1 & 0 & 0 & 0 & 0 & 1 & 0 & 0 \\ 0 & 0 & 0 & 0 & 1 & 0 & 0 & 0 & 0 & 0 & 0 \\ 0 & 0 & 0 & 0 & 0 & 1 & 0 & 0 & 0 & 0 & 0 \\ 0 & 0 & 0 & 0 & 0 & 0 & 0 & 0 & 0 & 0 & 0 \\ 0 & 0 & 0 & 0 & 0 & 0 & 1 & 1 & 0 & 0 & 0 \\ 0 & 0 & 0 & 0 & 0 & 0 & 0 & 0 & 0 & 1 & 0 \end{pmatrix}$$

$$\mathbf{Post}_{cc} = \begin{pmatrix} 0 & 0 & 0 & 0 & 0 & 0 & 0 & 0 & 0 & 0 & 0 \\ 1 & 0 & 0 & 0 & 0 & 0 & 0 & 0 & 0 & 0 & 0 \\ 0 & 0 & 1 & 0 & 0 & 0 & 0 & 1 & 0 & 0 & 0 \\ 0 & 1 & 0 & 1 & 0 & 0 & 0 & 0 & 0 & 0 & 0 \\ 0 & 0 & 0 & 0 & 1 & 0 & 0 & 0 & 0 & 0 & 0 \\ 0 & 0 & 0 & 0 & 0 & 1 & 1 & 0 & 0 & 0 & 0 \\ 0 & 0 & 0 & 0 & 0 & 0 & 0 & 0 & 1 & 1 & 0 \\ 0 & 0 & 0 & 0 & 0 & 0 & 0 & 0 & 0 & 0 & 1 \end{pmatrix}$$

While $\mathbf{Pre}_{cd} = \mathbf{Post}_{cd} = \mathbf{0}$, (22×22) matrices $\mathbf{Pre}_{dd}$, $\mathbf{Post}_{dd}$ as well as (22×11) matrices $\mathbf{Pre}_{dc}$, $\mathbf{Post}_{dc}$ are not introduced. Their entries are evident from Figure 8. Consider the discrete uniform probability distribution ${}^u f_x$ (3). Let the FOHPN continuous initial state be $\mathbf{x}_0^c = (100, 5, 10, 4, 2, 0, 5, 2)^T$ while the discrete initial state is $\mathbf{x}_0^d = (1, 0, 1, 0, 1, 0, 1, 0, 1, 0, 1, 0, 1, 0, 1, 0, 1, 0, 1, 0, 1, 0)^T$. Let the minimal speeds of the particular continuous transitions be $V_i^{min} = 0$ and let the maximal speeds be $V_i^{max} \in (11, 6, 6, 6, 11, 11, 3.7, 11, 6, 11, 11)$ (here is a small reserve against v_{ij} which were introduced above). The parameters of the probability distribution are $\mathbf{a} = (2, 2, 4, 4, 4, 4, 2, 2, 3, 3, 1, 1, 7, 7, 2, 2, 6, 6, 2, 2, 1, 1)$, $\mathbf{b} = (6, 6, 8, 8, 8, 8, 6, 6, 7, 7, 5, 5, 11, 11, 6, 6, 10, 10, 6, 6, 5, 5)$. The corresponding simulation results – the marking evolution of the continuous places P_i, $i = 1, \ldots, 6$ w.r.t. time – are given in Figure 9. The particular time functions are denoted there by the symbols $M(p_i)$, $i = 1, \ldots, 6$. Namely, as to the characters, the simulation tool HYPENS does not use capitals to denote the continuous places and transitions in order to distinguish them from the discrete ones. Firstly, the continuous places are numbered (starting from p_1) and then the numbering of the discrete places goes on from p_{n_c+1}, where n_c is the number of the continuous places. The same rule is applied in HYPENS at the numbering of the transitions.

Use now the deterministic timing of the discrete transitions, namely the following time delays $\Delta_{t_i} \in (4, 4, 6, 6, 6, 6, 4, 4, 5, 5, 2.5, 2.5, 9, 9, 4, 4, 8, 8, 4, 4, 2.5, 2.5)$. Apply here the same FOHPN model parameters except timing the discrete transitions. Then, the simulations results given in Figure 10 are achieved.

The graphical outputs of the simulation experiments yield the throughput of the particular roads in the transport network. They offer a useful view on the actual situation in the traffic. Thanks to the AGTTPM system, information about the alternative routes is at disposal for drivers practically on line. Thus, they can realize the flexible changes of the originally planned route, especially in case of a congestion. In case of the road transport, the deterministic timing of the FOHPN model is rather decisive, although the non-deterministic timing also helps to specify some details. At comparing Figures 9 and 10 it can be seen that the courses in Figure 10 are somewhat more continuous (especially at P_4) and smoothed, although the markings of the terminal places (P_6) are similar. The quantities of vehicles in corresponding places are indeed different, but not extremely. The simulation results achieved at ${}^e f_x$ were not introduced. Namely, for such kind of processes, ${}^u f_x$ it is more natural and more appropriate than ${}^e f_x$. Although a large area (city) cannot be modelled by a global model, it can be split into suitable segments (*agents*), and subsequently, the cooperation between the adjacent segments can be solved.

5 CASE STUDY ON FLEXIBLE MANUFACTURING SYSTEMS

For a mass production of hundreds (even thousands) parts the P/T PN model as well as the corresponding TPN model may be too large. Consequently, handling such

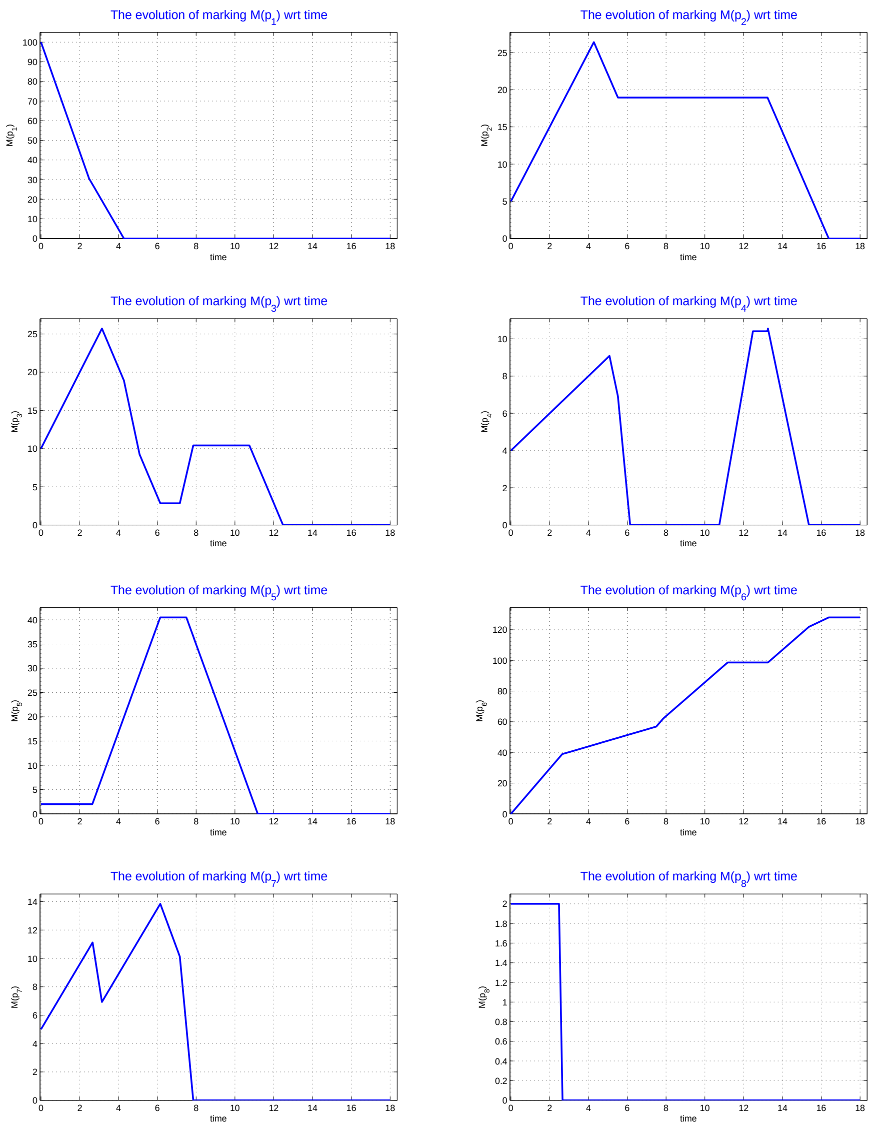

Figure 9. The evolution of the road transport in the locations P_1–P_8 w.r.t. time at the discrete uniform probability distribution of timing discrete transitions

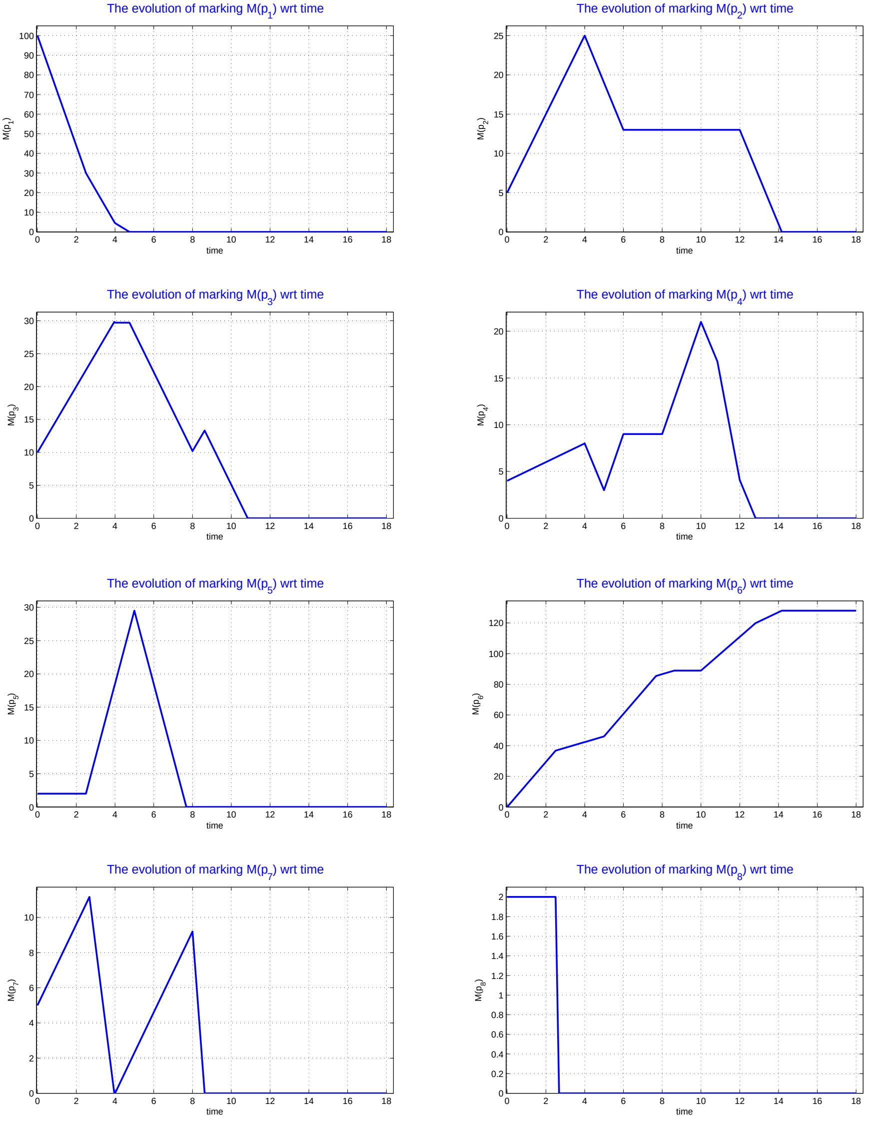

Figure 10. The evolution of the road transport in the locations P_1–P_8 w.r.t. time at the deterministic timing of the discrete transitions

models in the simulation process may be too tedious, even impossible. Therefore, let us utilize the FOHPN model. Consider the working station producing two kinds of the parts π_1 and π_2 on two parallel production lines L_1, L_2. Apply the FOHPN model given in Figure 11. The upper production line (L_1) produces the parts π_1 while the lower production line (L_2) produces the parts π_2. The machine tool is represented by p_5. It can produce both kinds of the parts, but not simultaneously, of course. The parts to be machined do not arrive into the system individually but in batches. In our case, the batches of 300 parts π_1 arrive into L_1 and the batches of 200 parts π_2 arrive into L_2. These batches are taken into account in Figure 11 by means of the weights of the input arcs of the continuous places P_1 (in $L1$) and P_4 (in $L2$) – see $\mathbf{Post}_{cd}$. The incidence matrices of the FOHPN model are the following:

$$\mathbf{Pre}_{cc} = \begin{pmatrix} 1 & 0 & 0 & 0 \\ 0 & 1 & 0 & 0 \\ 0 & 0 & 0 & 0 \\ 0 & 0 & 1 & 0 \\ 0 & 0 & 0 & 1 \\ 0 & 0 & 0 & 0 \\ 0 & 0 & 0 & 0 \\ 0 & 0 & 0 & 0 \end{pmatrix}$$

$$\mathbf{Post}_{cc} = \begin{pmatrix} 0 & 0 & 0 & 0 \\ 1 & 0 & 0 & 0 \\ 0 & 1 & 0 & 0 \\ 0 & 0 & 0 & 0 \\ 0 & 0 & 1 & 0 \\ 0 & 0 & 0 & 1 \\ 0 & 1 & 0 & 0 \\ 0 & 0 & 0 & 1 \end{pmatrix}$$

$$\mathbf{Pre}_{dc} = \mathbf{Post}_{dc} = \begin{pmatrix} 0 & 0 & 0 & 0 \\ 0 & 1 & 0 & 0 \\ 0 & 0 & 0 & 0 \\ 0 & 0 & 0 & 1 \\ 0 & 0 & 0 & 0 \\ 1 & 0 & 0 & 0 \\ 0 & 0 & 0 & 0 \\ 0 & 0 & 1 & 0 \\ 0 & 0 & 0 & 0 \\ 0 & 0 & 0 & 0 \\ 0 & 0 & 0 & 0 \end{pmatrix}$$

$$
\mathbf{Pre}_{cd} = \begin{pmatrix}
0 & 0 & 0 & 0 & 0 & 0 & 0 & 0 & 0 & 0 & 0 & 0 \\
0 & 0 & 5 & 0 & 0 & 0 & 0 & 0 & 0 & 0 & 0 & 0 \\
0 & 0 & 0 & 5 & 0 & 0 & 0 & 0 & 0 & 0 & 0 & 0 \\
0 & 0 & 0 & 0 & 0 & 0 & 0 & 0 & 0 & 0 & 0 & 0 \\
0 & 0 & 0 & 0 & 6 & 0 & 0 & 0 & 0 & 0 & 0 & 0 \\
0 & 0 & 0 & 0 & 0 & 6 & 0 & 0 & 0 & 0 & 0 & 0 \\
0 & 0 & 0 & 0 & 0 & 0 & 0 & 0 & 0 & 0 & 5 & 0 \\
0 & 0 & 0 & 0 & 0 & 0 & 0 & 0 & 0 & 0 & 0 & 6
\end{pmatrix}
$$

$$
\mathbf{Post}_{cd} = \begin{pmatrix}
300 & 0 & 0 & 0 & 0 & 0 & 0 & 0 & 0 & 0 & 0 & 0 \\
0 & 0 & 5 & 0 & 0 & 0 & 0 & 0 & 0 & 0 & 0 & 0 \\
0 & 0 & 0 & 0 & 0 & 0 & 0 & 0 & 0 & 0 & 0 & 0 \\
0 & 200 & 0 & 0 & 0 & 0 & 0 & 0 & 0 & 0 & 0 & 0 \\
0 & 0 & 0 & 0 & 6 & 0 & 0 & 0 & 0 & 0 & 0 & 0 \\
0 & 0 & 0 & 0 & 0 & 0 & 0 & 0 & 0 & 0 & 0 & 0 \\
0 & 0 & 0 & 0 & 0 & 0 & 0 & 0 & 0 & 0 & 0 & 0 \\
0 & 0 & 0 & 0 & 0 & 0 & 0 & 0 & 0 & 0 & 0 & 0
\end{pmatrix}
$$

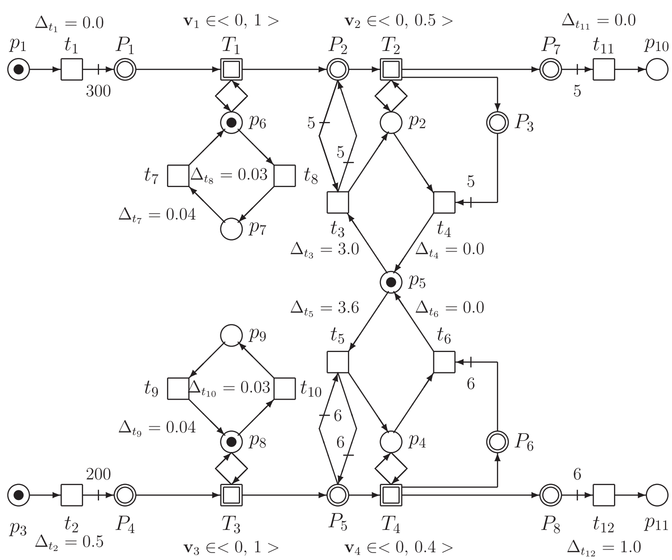

Figure 11. The FOHPN model of the manufacturing system

The binary matrices $\mathbf{Pre}_{dd}$ and $\mathbf{Post}_{dd}$ are evident from Figure 11. After the arrival of the batches into the lines, their parts are stored into the buffers – P_2 in $L1$ and P_5 in $L2$. The speed (IFS) of the continuous transition T_1 is $v_1 \in \langle 0, 1\rangle$ (in the number of parts per time unit), likewise the speed of T_3 is $v_3 \in 0, 1\rangle$. The speeds of the T_2 and T_4 are set up, respectively, on the values $v_2 \in \langle 0, 0.5\rangle$ and $v_4 \in \langle 0, 0.4\rangle$. The processing of the particular parts does not start immediately. Starting is delayed until the batches are stored into the buffers – at least 5 parts of type π_1 (see the weight of the arc $P_2 \to t_3$) into P_2 and 6 parts of type π_2 (see the weight of the arc $P_5 \to t_5$) into P_5. Then, the uploading of the machine can be done once more. Suppose that the machining of the parts π_1 takes 3.0 time units while the machining of the parts π_2 takes 3.6 time units. In the deterministic case, they represent the time delays of the transitions t_3 and t_5. Therefore, $\Delta_{t_3} = 3.0$ while $\Delta_{t_5} = 3.6$. Other discrete transitions have the delays set up as follows: $\Delta_{t_1} = 0.0$ as well as Δ_{t_4}, Δ_{t_6} and $\Delta_{t_{11}}$, $\Delta_{t_2} = 10.0$, $\Delta_{t_7} = 0.04$ as well as Δ_{t_9}, $\Delta_{t_8} = 0.03$ as well as $\Delta_{t_{10}}$, $\Delta_{t_{12}} = 1.0$. After processing all of the parts in the batch, the machine is prepared to process another batch. The machined pieces are removed from buffers also in the batches having the input size (i.e. 5 parts π_1 and 6 parts π_2). The fired continuous transitions T_1, T_2, T_3 and T_4 approximate the discrete movement of the parts by the continuous flows. Consequently, the model dimensionality and especially the simulation time are extensively reduced. The replacement of the discrete PN model by the FOHPN model makes the analysis of the real FMS simplier. Thus, the FOHPN models, primarily determined for modelling the systems hybrid by nature (HS), can be used also for modelling some of the pure DES. As it was demonstrated, in case of the mass production they can be exploited also for modelling of the batch processes.

Till now the deterministic case was analysed. The corresponding results introduced in Figure 12 show that the machine processes only batches of the same kind. Namely, first the batches of the production line $L1$ are processed and then the batches of $L2$.

Try now to use the non-deterministic model and test whether the alternative processing of different batches is possible or not. Consider e.g. ${}^{e}f_x$ (3) for timing the discrete transitions with $\lambda_i \in (0.001, 1.0, 0.3, 0.001, 0.36, 0.001, 0.04, 0.03, 0.04, 0.03, 0.001, 0.1)$. Other parameters of the model are the same. The simulation results of the experiment introduced in Figure 13 show that *theoretically* the machine is able to alternate the batches from both lines. It is apparent from the comparison of the corresponding markings in both figures. While in Figure 12 the markings fluently accrue/descend, in Figure 13 they accrue/descend roughly. It is caused by alternating the lines. However, production time of the lines in Figure 13 is shorter by about 30 percents compared to Figure 12. But, applicability has to be verified in practice.

6 WF OF EVACUATION OF EA

The evacuation of people from EA is of first-rate importance. It is the principal matter. Although crisis situations cannot be completely controlled, they can be at least partially influenced. In order to manage the evacuation process, first of all the flexible escape strategies have to be found as well as the safe and free escape routes. Suitable models can yield useful information, especially in the process of simulation. The WF of the evacuation is also very important.

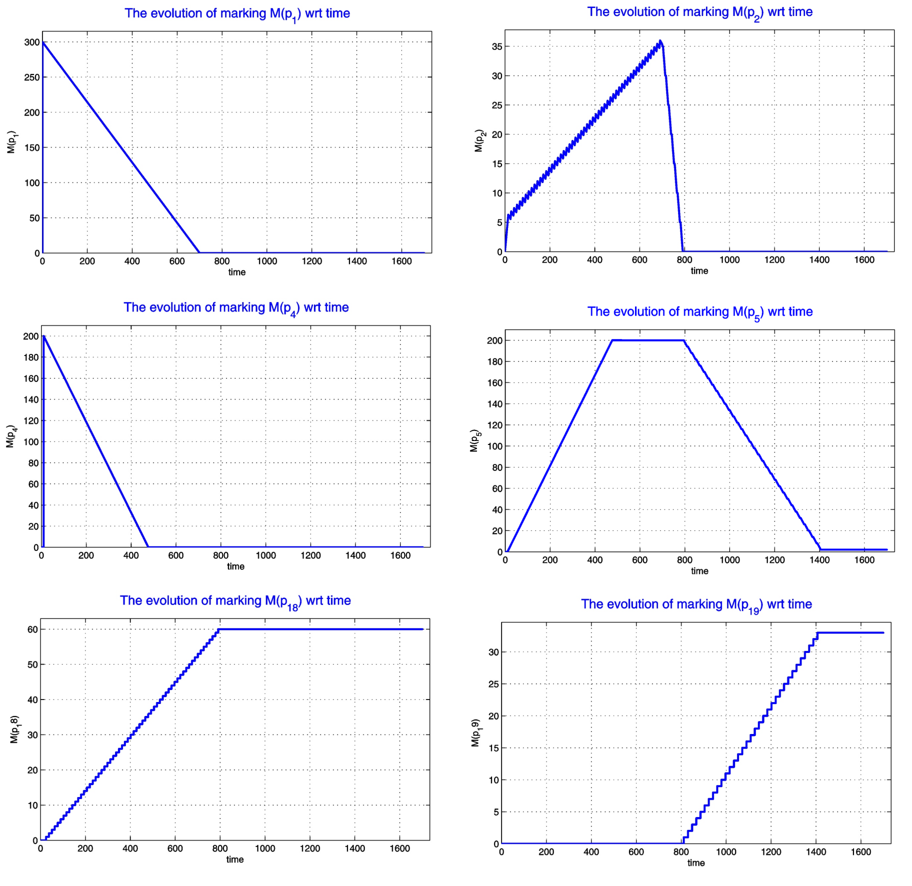

Figure 12. The simulation results for the deterministic timing the FOHPN discrete transitions. In the particular pictures the marking evolution of the FOHPN continuous places P_1, P_2, P_4, P_5 and the discrete places p_{10}, p_{11} (being, respectively, the stacks of the finished parts π_1, π_2) w.r.t. time is displayed

P/T PN are suitable for modelling EA by means of the modular approach. Especially, the structure modules (agents, subsystems) can be utilized. Consider EA being a part of a building schematically outlined in Figure 14. In a crisis situation it is necessary to evacuate people from the rooms $R1$–$R4$ and from the corridor $R5$ to a safe space through the exits $E1$–$E3$.

The rooms $R1$, $R3$ have, respectively, only the doors $D1$, $D3$ directing to the corridor $R5$. The main exit $E1$ leads from the corridor R_5 to the safe space out of EA. Each of the rooms $R2$, $R4$ has two doors. Namely, $R2$ has the door D_2 to the corridor R_5 and the exit E_2 to the safety, while R_4 has the door D_4 to R_5 and the exit E_3 to the safety. Consequently, the crowd may tend from R_5 not

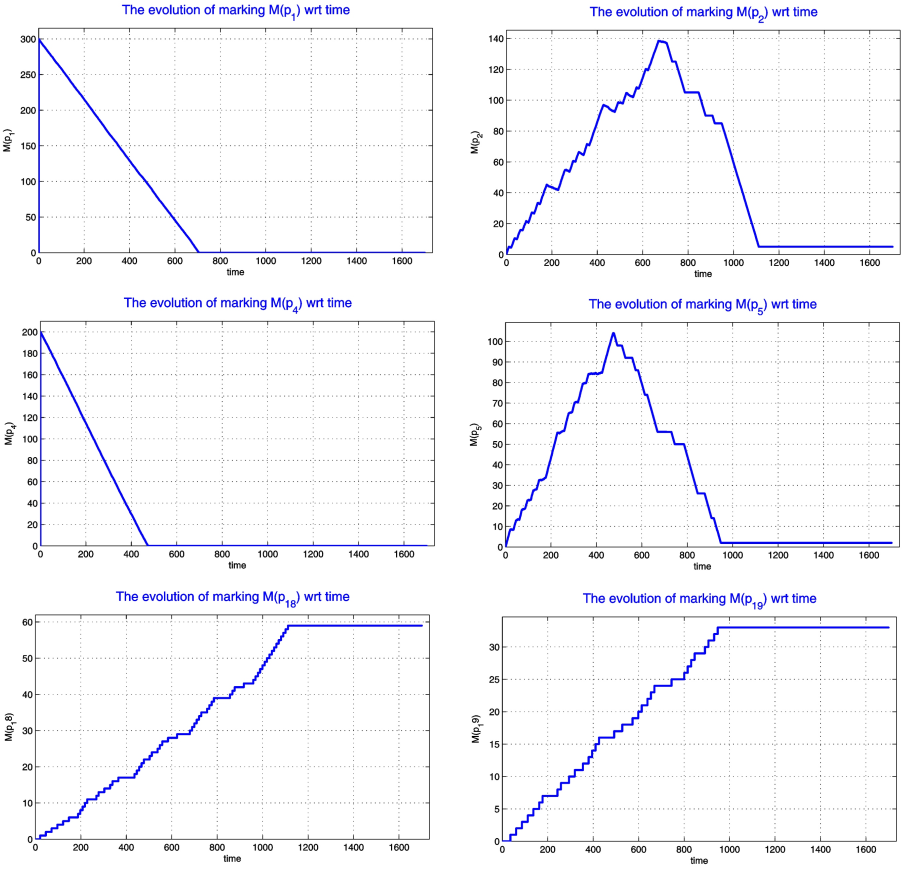

Figure 13. The simulation results for the exponential probability distribution of timing the FOHPN discrete transitions. In the particular pictures the marking evolution of the FOHPN continuous places P_1, P_2, P_4, P_5 and the discrete places p_{10}, p_{11} (being, respectively, the stacks of the finished parts π_1, π_2) w.r.t. time is displayed.

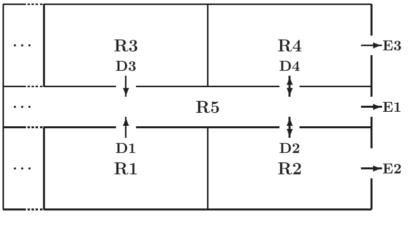

Figure 14. The scheme of the EA

only to E_1 but also from R_5 to $R2$ or $R4$. When the rooms and the corridor are modelled by means of the P/T PN places and the doors and exits are modelled by means of the P/TPN sub-nets, the P/T PN model displayed in Figure 15 can be built.

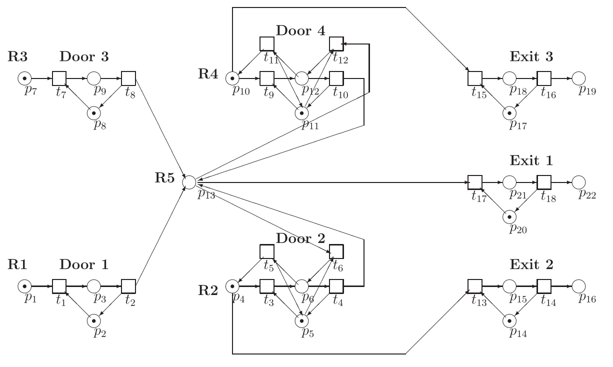

Figure 15. The P/T PN-based model of the EA

The doors can be understood to be agents, at least the passive agents [21]. In [8] the supervision theory was applied to this P/T PN model of EA in order to force the rules of its behaviour. More details about the P/T PN-based synthesizing the supervisors can be found in [8]. The P/T PN-based model of the evacuation WF was investigated in [9]. Here, the TPN model and the FOHPN one are utilized to this purpose.

Inspect here the approach modelling WF of the evacuation process by means of TPN and FOHPN.

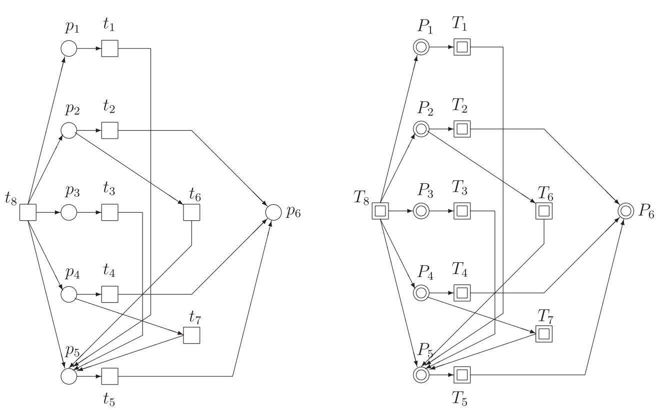

Figure 16. The models of WF of the evacuation process: the TPN-based model (left) and the FOHPN-based model (right)

The TPN-based model of WF as well as the FOHPN-based one are depicted in Figure 16. As to the structure, the WF models are simpler than the models respecting almost exactly the physical features of EA (compare Figure 15 with Figure 14 as well as Figure 16 with Figure 15). The sense of the WF places and transitions is somewhat different in spite of the following facts. The places p_1–p_5 and/or P_1–P_5 in Figure 16 also represent the rooms $R1$–$R4$ and the corridor R_5 to be evacuated. The transitions t_1, t_3, t_6, t_7 and/or T_1, T_3, T_6, T_7 also represent the routes (doors) to the corridor and t_2, t_4, t_5 and/or T_2, T_4, T_5 also represent the routes (exits) to the safe space. However, the PN model of the doors is missing. Moreover, p_6 and/or P_6 express the safe space and t_8 and/or T_8 formally express the start of WF. There are many intuitive aspects which can be applied at the modelling and analysis of WF – see [32] where WIFA (A Workflows Intuitive, yet Formal Approach) is presented.

Moreover, the simple TPN model of WF introduced in Figure 16 (left) can be completed by a kind of the supervisor(s). Especially, the question about how to resolve the conflicts on the outputs from the places p_2 and p_4 intrudes. Predefining the priority between the output arcs of p_2 as well as the one between the output arcs of p_4 may resolve the problem. The conditions concerning the priorities between the alternative escape routes can be expressed by means of the components of the Parikh's vector e.g. as follows: $v_2 > v_6$ and $v_4 > v_7$. It means that the escape routes directed immediately from p_2 and p_4 to the safe space are preferred before the routes directed to the corridor. Thus, for the initial Parikh's vector $\mathbf{v}_0 = \mathbf{0}$ it results from (15) that

$$\mathbf{L}_v = \begin{pmatrix} 0 & -1 & 0 & 0 & 0 & 1 & 0 & 0 \\ 0 & 0 & 0 & -1 & 0 & 0 & 1 & 0 \end{pmatrix} \qquad \mathbf{b} = \begin{pmatrix} 0 \\ 0 \end{pmatrix} \qquad \mathbf{x}_0^s = \begin{pmatrix} 0 \\ 0 \end{pmatrix}$$

$$\mathbf{F}_s = \begin{pmatrix} 0 & 0 & 0 & 0 & 0 & 1 & 0 & 0 \\ 0 & 0 & 0 & 0 & 0 & 0 & 1 & 0 \end{pmatrix} \qquad \mathbf{G}_s^T = \begin{pmatrix} 0 & 1 & 0 & 0 & 0 & 0 & 0 & 0 \\ 0 & 0 & 0 & 1 & 0 & 0 & 0 & 0 \end{pmatrix}$$

The supervisor with the structure $\mathbf{F}_s$, $\mathbf{G}_s^T$ and the initial state $\mathbf{x}_0^s$, obtained by (16)–(18), ensures that the desired strategy is done. For other combinations of the priorities $v_2 < v_6$ and $v_4 < v_7$; $v_2 > v_6$ and $v_4 < v_7$; $v_2 < v_6$ and $v_4 > v_7$ the supervisors will be different for each combination. In the non-deterministic cases the problem of the priorities is automatically (but randomly, of course) resolved. This is more realistic than the constantly prescribed priorities. Moreover, the parameters of the particular probability distributions of timing the transitions can be set up in the dependency upon the assumed behaviour of the crowd escaping from EA.

6.1 TPN Modelling Evacuation WF

The structural parameters of the TPN model depicted in Figure 16 (left) are

$$\mathbf{Pre} = \begin{pmatrix} 1 & 0 & 0 & 0 & 0 & 0 & 0 & 0 \\ 0 & 1 & 0 & 0 & 0 & 1 & 0 & 0 \\ 0 & 0 & 1 & 0 & 0 & 0 & 0 & 0 \\ 0 & 0 & 0 & 1 & 0 & 0 & 1 & 0 \\ 0 & 0 & 0 & 0 & 1 & 0 & 0 & 0 \\ 0 & 0 & 0 & 0 & 0 & 0 & 0 & 0 \end{pmatrix}$$

$$\mathbf{Post} = \begin{pmatrix} 0 & 0 & 0 & 0 & 0 & 0 & 0 & 1 \\ 0 & 0 & 0 & 0 & 0 & 0 & 0 & 1 \\ 0 & 0 & 0 & 0 & 0 & 0 & 0 & 1 \\ 0 & 0 & 0 & 0 & 0 & 0 & 0 & 1 \\ 1 & 0 & 1 & 0 & 0 & 1 & 1 & 1 \\ 0 & 1 & 0 & 1 & 1 & 0 & 0 & 0 \end{pmatrix} \qquad (19)$$

In both cases (deterministic and non-deterministic), the time specifications have to be found either experimentally or by a guesswork (i.e. by a qualified estimate). Namely, on the one hand they depend on the physical parameters of the corresponding routes and gate-ways determining their throughput (e.g. their shape, dimension, etc.), and on the other hand they depend on the psychological aspects of the people behaviour in a crowd during the escape from a danger to safety. In case of the routes leaving EA through the corridor the time specifications depend also on the physical length of the corridor. Because the transition t_8 in the TPN model has only a symbolic importance (starting the WF process), it can be omitted.

Consider the deterministic case with the following time delays (in time unit) assigned to the TPN transitions: $\Delta_{t_1} = 20$, $\Delta_{t_2} = 25$, $\Delta_{t_3} = 20$, $\Delta_{t_4} = 25$, $\Delta_{t_5} = 30$, $\Delta_{t_6} = 25$, $\Delta_{t_7} = 20$. The markings of the particular places (p_1–p_4 representing the rooms, p_5 representing the corridor and p_6 representing the safe space) express the number of humans in the corresponding localities. Consider that at the beginning of the evacuation process they are expressed by $\mathbf{x}_0 = (10, 30, 15, 40, 5, 0)^T$. The achieved simulation results are in Figure 17.

Inspect now the non-deterministic cases. Consider firstly ${}^e f_x$ (3) for timing discrete transitions. Let the parameters λ_1–λ_7, be the entries of the vector $\lambda = 20.(2, 2.5, 2, 2.5, 3, 2.5, 2.5)$, belong to the TPN transitions t_1–t_7. Other model parameters and the initial state are the same as those used in the deterministic case. The marking evolution of $p_1 - p_6$ w.r.t. time is displayed in Figure 18.

Now, consider ${}^u f_x$ (3) for timing the transitions. Let the parameters a_i, b_i, $i = 1, \ldots, 7$, be the corresponding entries of the vectors $\mathbf{a} = 20.(.1, .1, .1, .1, .1, .1, .1)$ and $\mathbf{b} = 20.(2, 3, 2, 3, 2, 3, 3)$. Other parameters of the TPN model are the same as those used at ${}^e f_x$. The achieved marking evolution of $p_1 - p_6$ w.r.t. time is displayed in Figure 19.

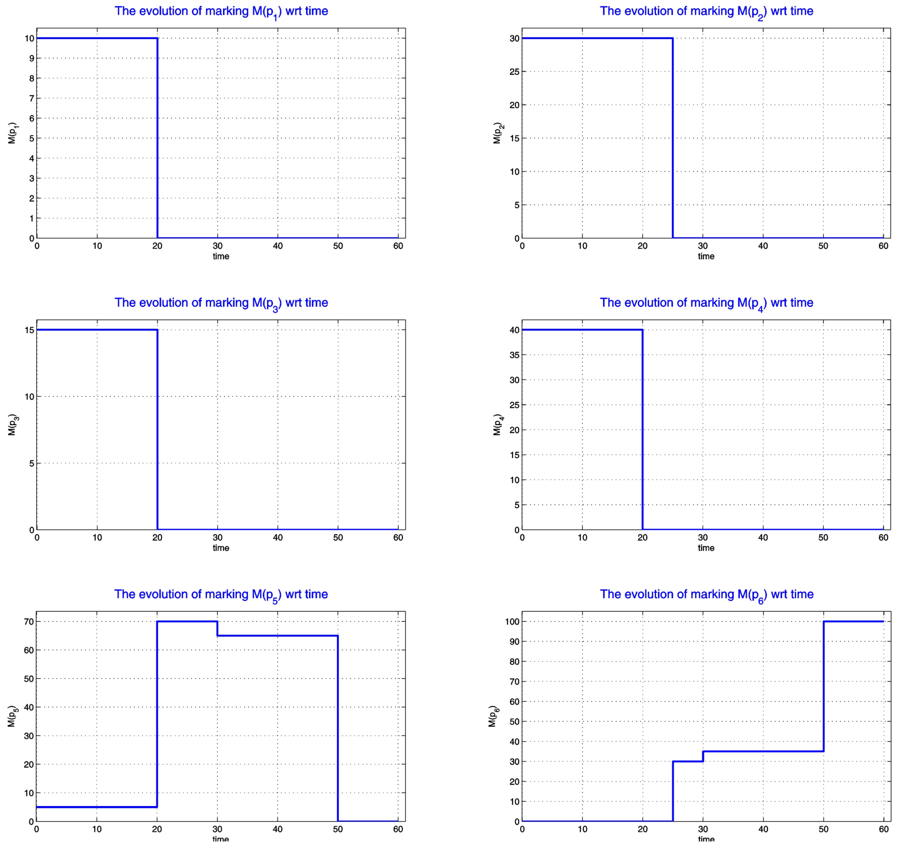

Figure 17. The simulation results achieved by means of the TPN model at the deterministic timing the transitions. The marking evolution of the places p_1–p_6 w.r.t. time.

Figures 17–19 show that TPN yield rather information about the global time necessary for the exhausting of the rooms, corridor and the whole EA than comprehensive information about the gradual emptying/filling the particular spaces. Perhaps, only the markings of p_5 and p_6 exhibit certain gradual changes. Comparing Figures 17–19 we can see that the fundamental features of the results are more or less analogical.

6.2 FOHPN at Modelling of Evacuation WF

Consider the FOHPN model of the evacuation WF. In this case it is also advisable to eliminate the continuous transition T_8 occurring in Figure 16 (right). Thus, the matrices $\mathbf{Pre}_{cc}$, $\mathbf{Post}_{cc}$ have the same form as those in (19) without the 8$^{\text{th}}$

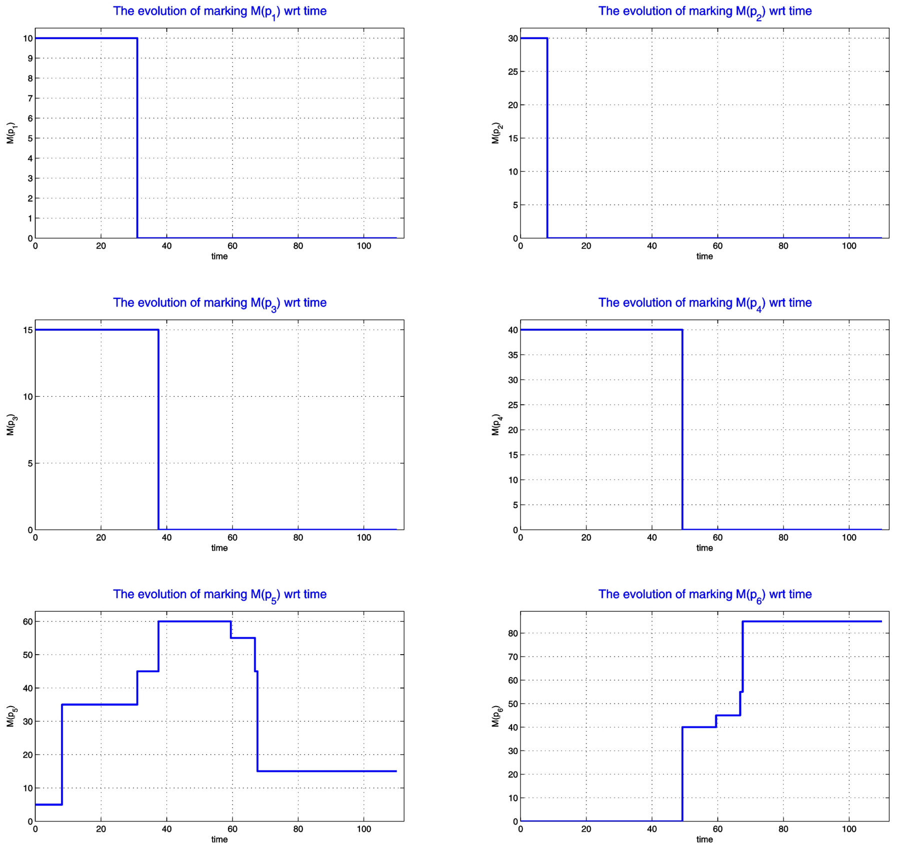

Figure 18. The simulation results achieved by means of the TPN model at the exponential probability distribution of timing the transitions. The marking evolution of the places p_1–p_6 w.r.t. time.

columns. $\mathbf{Pre}_{cd} = \mathbf{Post}_{cd} = \mathbf{0}/_{(6\times 14)}$, $\mathbf{Pre}_{dc} = \left[\text{blockdiag}\,({}^1\mathbf{M}_i)_{i=1,7}\right] = \mathbf{Post}_{dc}$, $\mathbf{Pre}_{dd} = \left[\text{blockdiag}\,({}^2\mathbf{M}_i)_{i=1,7}\right]$, $\mathbf{Post}_{dd} = \mathbf{I}_{(14\times 14)}$. Namely, ${}^1\mathbf{M}_i$, ${}^2\mathbf{M}_i$ are related to the control module displayed in Figure 8 (right).

Start the deterministic case from the initial marking $\mathbf{x}_0^c = (10, 30, 15, 40, 5, 0)$ of the continuous places. Let the minimal speeds of $T_j, j = 1, \ldots, 7$, be $V_j^{min} = 0.0$ and their maximal speeds V_j^{max} be the entries of the vector $\mathbf{V}^{max} = 0.01.(22, 32, 25, 30, 50, 14, 17)$. Let $\Delta_j \in [100.(1, 2, 1, 2, 1, 2, 1, 2, 1, 2, 1, 2, 1, 2)]$ be the deterministic timing of the discrete transitions in the control modules for T_j. The achieved marking evolution of the continuous places w.r.t. time is in Figure 20.

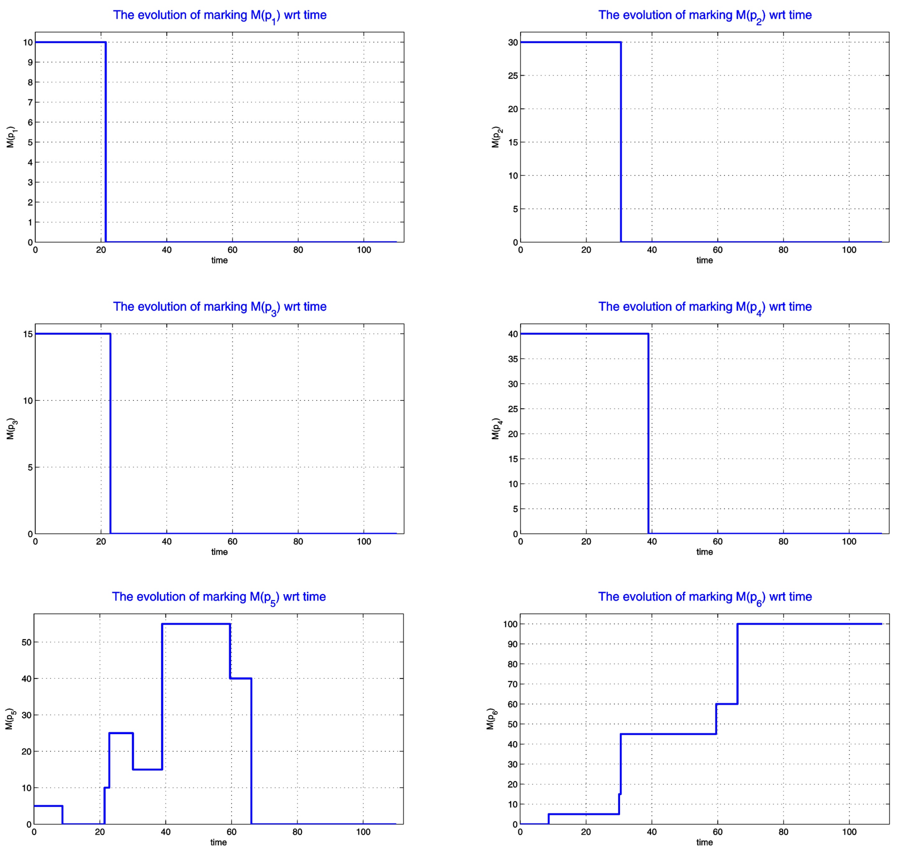

Figure 19. The simulation results achieved by means of the TPN model at the discrete uniform probability distribution of timing the transitions. The marking evolution of the places $p_1 - p_6$ w.r.t. time.

Inspect now the non-deterministic timing. Consider firstly ${}^u f_x$ at timing the discrete transitions. Let the parameters be $a_j = 0.09$, $j = 1, \ldots, 14$, $b_j = 90$ for odd j and $b_j = 180$ for even j, $j = 1, \ldots, 14$. The initial state $\mathbf{x}_0^c$ and the speed parameters of the continuous transitions are the same as in the deterministic case. The marking evolution of the continuous places P_i, $i = 1, \ldots, 6$, is given in Figure 21.

In case of the exponential probability distribution consider λ_i, $i = 1, \ldots, 14$, being the entries of the vector $\lambda = 100.(1, 2, 1, 2, 1, 2, 1, 2, 1, 2, 1, 2, 1, 2)$. The initial state $\mathbf{x}_0^c$, the limit IFS values of the continuous transitions, and other parameters are the same as in the previous case. Thus, we obtain the marking evolution of the continuous places given in Figure 22.

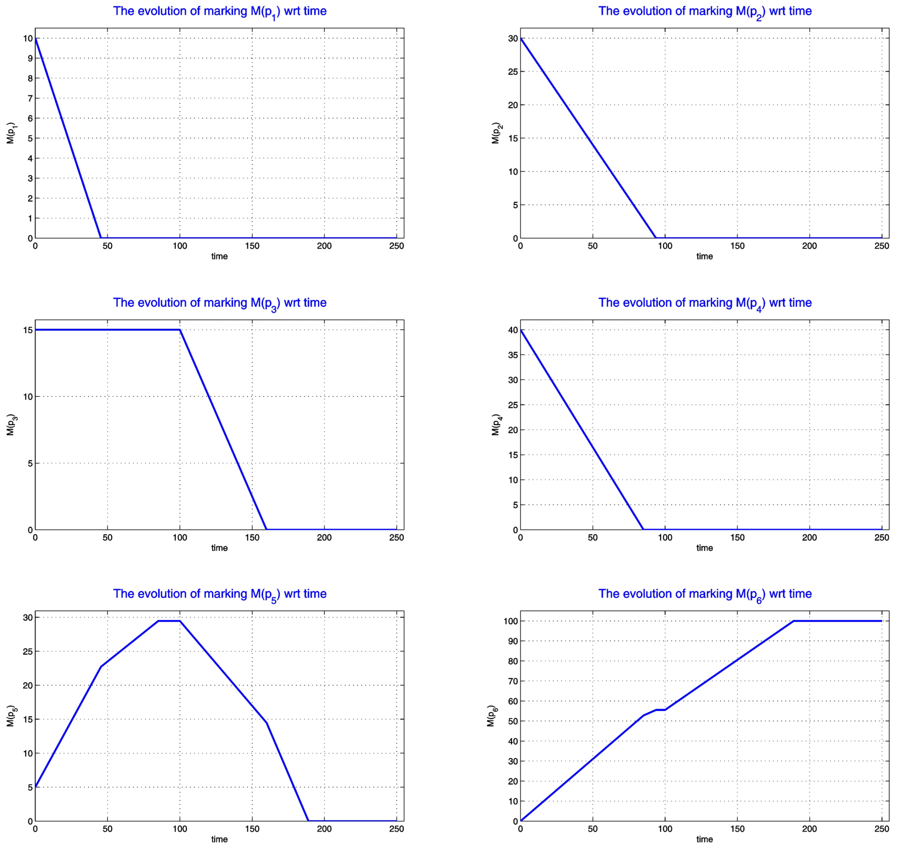

Figure 20. The simulation results achieved by means of the FOHPN model at the deterministic timing the discrete transitions. The evolution of markings of the continuous places P_1–P_6 w.r.t. time.

The simulation results based on the FOHPN model of WF presented in Figures 20–22 yield dynamics of exhausting and/or filling of all spaces (i.e. the rooms, corridor and safe space). Comparing the figures we can see an analogy among the marking evolutions of the corresponding FOHPN continuous places. However, in the non-deterministic cases, filling/exhausting the corridor and filling the safe space is smoother and more continuous than in the deterministic case.

7 CONCLUSION

The main idea of this paper is to point out the possibilities of modelling, analysing and supervisory control of the DES and HS. In contrast to previous works where

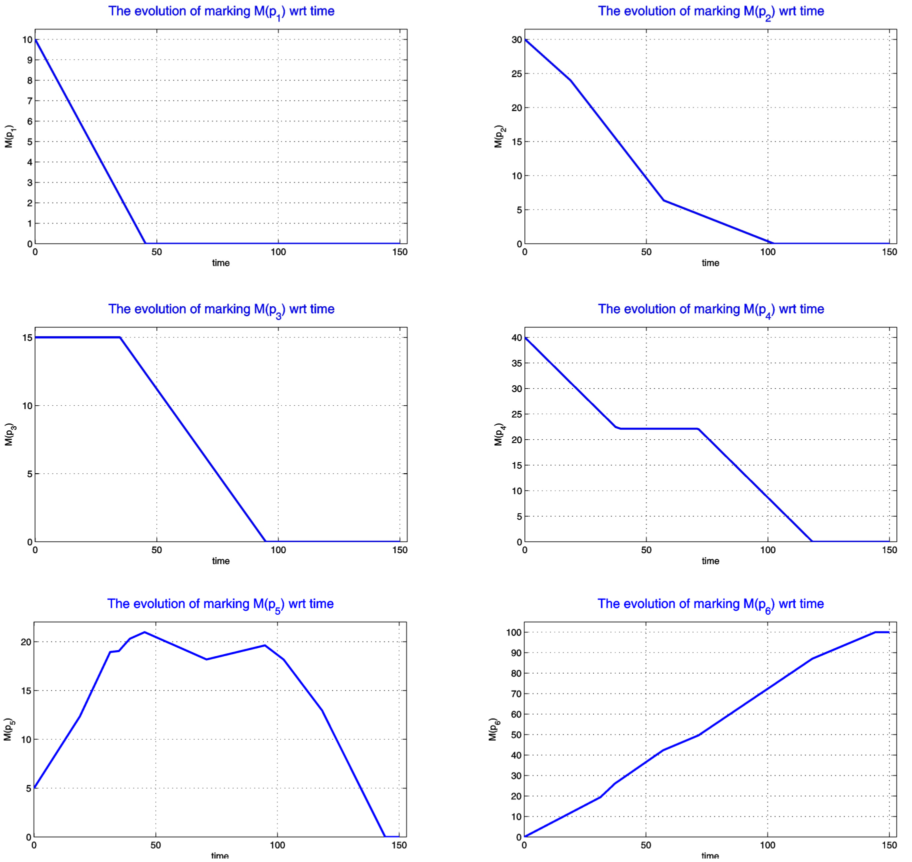

Figure 21. The simulation results achieved by means of the FOHPN model at the discrete uniform probability distribution of timing the discrete transitions. The marking evolution of P_1–P_6 with respect to time.

P/T PN were utilized, here the TPN and FOHPN were applied. Consequently, the time behaviour can be observed. Four case studies were introduced.

The cooperation among the modules (agents), being the principle of the computational collective intelligence, is realized here by means of the organized passing of

1. vehicles on the rails and/or roads;
2. the parts or their batches through the production lines of FMS;
3. people through escape routes from EA to safety.

Often, the supervisor (serving as the agent-organizer) has to be synthesized. The mathematical background for this was introduced in (4)–(18).

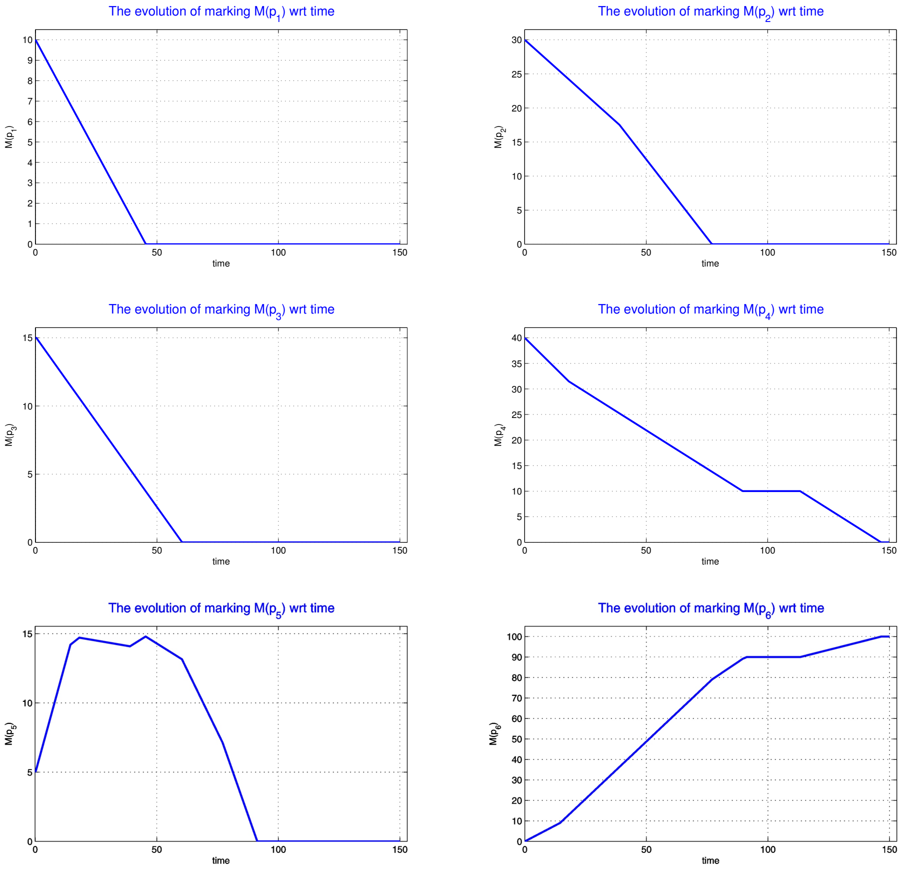

Figure 22. The simulation results achieved by means of the FOHPN model at the exponential probability distribution of timing the discrete transitions. The marking evolution of P_1–P_6 with respect to time.

To verify the soundness of the approach, a lot of simulations were performed. Naturally, all of the results cannot be introduced here because of the limited space. Some of the simulation results were presented, compared and discussed. The results corroborate applicability of the proposed approach. The approach is sufficiently general and therefore it can be used also in many other areas.

While in the P/T PN models the time specifications are missing, in the TPN and FOHPN models they can be applied in a wide range. Thus, the throughput and the performance evaluation of the systems were obtained. Two kinds of timing the discrete transitions were used here – deterministic and non-deterministic.

The presented approach proves that

1. the supervision is a powerful technique that can be used in practice;
2. TPN and FOHPN are flexible models which allow to model non-trivial case studies;
3. sometimes, especially in mass production, FOHPN models reduce the number of states occurring in P/T PN models;
4. HYPENS is a good software tool supporting these kinds of analysis DES and HS;
5. comparison the TPN and HPN models with other kinds of models presented e.g. in [22] and [32] should not be confrontational but rather cooperative.

Namely, the models support each other in spite of their different origins as it was shown at usage AGTTPM in the Section 4 or in case of WIFA in the Section 6.

On the other hand, the process of PN-based modelling is mostly intuitive. To some extent it depends on knowledge and experience of the model builder. However, the research concerning the TPN and FOHPN modelling has to be closely linked with real systems to be modelled. Namely, the acquisition of model parameters is very important too. Especially, the FOHPN models contain a lot of parameters. Moreover, setting some of them in the process of simulation is sometimes laboured, particularly in non-deterministic cases. Therefore, further research is needful in these directions.

Acknowledgement

The author thanks for the partial support of the VEGA agency (under Grant No. 2/0039/13) and the ERDF agency (under Grants ITMS 26240220064 and ITMS 26240220060).

REFERENCES

[1] van der Aalst, W. M. P.: Workflow Verification: Finding Control-Flow Errors Using Petri Net-Based Techniques. In: van der Aalst, W. M. P., Desel, J., Oberweis, A. (Eds.): Business Process Management. Models, Techniques, and Empirical Studies, Springer-Verlag, Berlin-Heidelberg, LNCS, Vol. 1806, 2000, pp. 161–183.

[2] van der Aalst, W. M. P.—van Hee, K. M.: Workflow Management: Models, Methods, and Systems. MIT Press, Cambridge, MA, USA, 2004.

[3] Balduzzi, F.—Giua, A.—Menga, G.: First-Order Hybrid Petri Nets: A Model for Optimization and Control. IEEE Transactions on Robotics and Automation, Vol. 16, 2000, No. 4, pp. 382–399.

[4] Balduzzi, F.—Giua, A.—Seatzu, C.: Modelling and Simulation of Manufacturing Systems Using First-Order Hybrid Petri Nets. International Journal of Production Research, Vol. 39, 2001, No. 2, pp. 255–282.

[5] Balduzzi, F.—Di Febbraro, A.—Giua, A.—Seatzu, C.: Decidability Results in First-Order Hybrid Petri Nets. Discrete Event Dynamic Systems: Theory and Applications, Vol. 11, 2001, No. 1-2, pp. 41–57.

[6] Čapkovič, F.: Modelling, Analysing and Control of Interactions among Agents in MAS. Computing and Informatics, Vol. 26, 2007, No. 5, pp. 507–541.

[7] Čapkovič, F.: Automatic Control Synthesis for Agents and their Cooperation in MAS. Computing and Informatics, Vol. 29, 2010, No. 6+, pp. 1045–1071.

[8] Čapkovič, F.: Supervision of Agents Modelling Evacuation at Crisis Situations. In: Jezic, G., Kusek, M., Nguyen, N. T., Howlett, R. J., Jain, L. C. (Eds.): Agent and Multi-Agent Systems. Technologies and Applications, Springer-Verlag, Berlin-Heidelberg, LNAI, Vol. 7327, 2012, pp. 24–33.

[9] Čapkovič, F.: Modelling Evacuation at Crisis Situations by Petri Net-Based Supervision. In: Nguyen, N. T. (Ed.): Transactions on Computational Collective Intelligence XII, Springer-Verlag, Berlin-Heidelberg, LNCS, Vol. 8240, 2013, pp. 143–170.

[10] Čapkovič, F.: Travel Routes Flexibility in Transport Systems. In: Barbucha, D., Le, M. T., Howlett, R. J., Jain, L. C. (Eds.): Advanced Methods and Technologies for Agent and Multi-Agent Systems. IOS Press, Amsterdam-Berlin-Tokyo-Washington DC, 2013, pp. 30–39.

[11] Čapkovič, F.: Petri Net-Based Approach to Modelling ATM and Minimising Logistic Costs in ATM Network. International Journal of Computational Intelligence Studies, Vol. 2, 2013, Nos. 3/4, pp. 202–217.

[12] Čapkovič, F.: Agent-Based Modelling the Evacuation of Endangered Areas. In: Nguyen, N. T., Attachoo, B., Trawiński, B., Somboonviwat, K. (Eds.): Intelligent Information and Database Systems, Springer-Verlag, Berlin-Heidelberg, LNAI, Vol. 8397, 2014, pp. 281–290.

[13] Čapkovič, F.: Modelling Travel Routes in Transport Systems by Means of Timed and Hybrid Petri Nets. In: Jezic, G., Kusek, M., Lovrek, I., Howlett, R.J., Jain, L. C. (Eds.): Agent and Multi-Agent Systems: Technologies and Applications, Springer, Advances in Intelligent Systems and Computing, Vol. 296, 2014, pp. 97–106.

[14] Čapkovič, F.: Agent-Based Modelling of the Evacuation of Endangered Areas in Crisis Situations. Vietnam J. of Computer Science, Vol. 2, 2015, No. 1, pp. 35–45.

[15] David, R.—Alla, H.: On Hybrid Petri Nets. Discrete Event Dynamic Systems: Theory and Applications, Vol. 11, 2001, No. 1-2, pp. 9–40.

[16] Desel, J.—Reisig, W.: Place/Transition Petri Nets. In: Reisig, W., Rozenberg, G. (Eds.): Lectures on Petri Nets I: Basic Models. Advances in Petri Nets, Springer-Verlag, Berlin-Heidelberg, LNCS, Vol. 1491, 1989, pp. 122–173.

[17] Dotoli, M.—Fanti, M.—Iacobellis, G.—Mangini A. M.: A First-Order Hybrid Petri Net Model for Supply Chain Management, IEEE Transactions on Automation Science and Engineering, Vol. 6, 2009, No. 4, pp. 744–758.

[18] Iordache, M. V.—Antsaklis, P. J.: Supervision Based on Place Invariants: A Survey. Discrete Event Dynamic Systems: Theory and Applications, Vol. 16, 2006, No. 4, pp. 451–492.

[19] Iordache, M. V.—Antsaklis, P. J.: Supervisory Control of Concurrent Systems: A Petri Net Structural Approach. Birkhäuser, Boston, 2006.

[20] IORDACHE, M. V.: Methods for the Supervisory Control of Concurrent Systems Based on Petri Nets Abstraction. Ph.D. Dissertation, University of Notre Dame, Notre Dame, Indiana, USA, 2003.

[21] KUBERA, Y.—MATHIEU, P.—PICAULT, S.: Everything Can be Agent! In: van der Hoek, W., Kaminka, G. A., Lespérance, Y., Luck, M., Sen, S. (Eds.): Proceedings of the 9th International Conference on Autonomous Agents and Multiagent Systems (AAMAS '10), Toronto, Canada, May 2010, pp. 1547–1548.

[22] LIU, Y.—DAI, Y.—DAI, Z.: Real-Time Adaptive Gray Threshold Measurement in Extracting Traffic Parameters. International Journal of Innovative Computing, Information and Control, Vol. 6, 2010, No. 4, pp. 1583–1594.

[23] MURATA, T.: Petri Nets: Properties, Analysis and Applications. Proceedings of the IEEE, Vol. 77, 1989, No. 4, pp. 541–580.

[24] PETERSON, J. L.: Petri Nets Theory and the Modelling of Systems. Prentice-Hall Inc., Englewood Cliffs, New York, 1981.

[25] PETRI, C. A.: Communication with Automata. Technical Report RADC-TR-65-377, Vol. 1. Available on: `http://www.dtic.mil/dtic/tr/fulltext/u2/630125.pdf`, 1966.

[26] POPOVA-ZEUGMANN, L.: Time Petri Nets: Theory, Tools and Applications, Part 1, Part 2. Available on: `http://www2.informatik.hu-berlin.de/~popova/1-part-short.pdf`, `http://www2.informatik.hu-berlin.de/~popova/2-part-short.pdf`, 2008.

[27] QU, Y.—LI, L.—YAN, L.—CHEN, Y.—DAI, Y.: Travel Routes Estimation in Transportation Systems Modeled by Petri Nets. Proceedings of the 2010 IEEE International Conference on Vehicular Electronics and Safety (ICVES 2010), QingDao, China, July 2010, pp. 73–77.

[28] REISIG, W.: Petri Nets. An Introduction. Springer, Berlin-Heidelberg, 1985.

[29] SESSEGO, F.—GIUA, A.—SEATZU, C.: HYPENS: A Matlab Tool for Timed Discrete, Continuous and Hybrid Petri Nets. In: van Hee, K. M., Valk, R. (Eds.): Applications and Theory of Petri Nets, Springer, Berlin-Heidelberg-New York, LNCS, Vol. 5062, 2008, pp. 419–428.

[30] SESSEGO, F.—GIUA, A.—SEATZU, C.: HYPENS Manual. Available on: `http://www.diee.unica.it/automatica/hypens/Manual_HYPENS.pdf`, 2008.

[31] WANG, J.: Timed Petri Nets. Kluwer Academic Publishers, Boston, MA, USA, 1998.

[32] WANG, J.—ROSCA, D.—TEPFENHART, W.—MILEWSKI, A.: Incident Command System Workflow Modeling and Analysis: A Case Study. In: van de Walle, B., Turoff, M. (Eds.): Proceedings of the 3rd International ISCRAM Conference, Newark, NJ, USA, May 2006, p. 127–136.

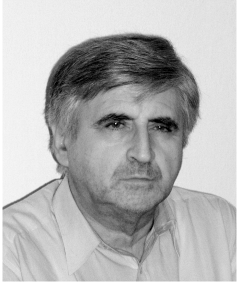

František Čapkovič received his M.Sc. degree in 1972 from the Faculty of Electrical Engineering of the Slovak Technical University, Bratislava, Slovakia. Since 1972 he has been working with the Slovak Academy of Sciences (SAS), Bratislava, namely in 1972–1991 at the Institute of Technical Cybernetics, in 1991–2001 at the Institute of Control Theory and Robotics and from 2001 till now at the Institute of Informatics. In 1980 he received the Ph.D. degree from SAS. Since 1998 he has been Associate Professor. He works in the area of modelling, analysing and intelligent control of discrete-event systems (DES) and hybrid systems. He is the author of more than 200 publications.